Cell Stem Cell
Article

Transient Inactivation of *Rb* and *ARF* Yields Regenerative Cells from Postmitotic Mammalian Muscle

Kostandin V. Pajcini,[1] Stephane Y. Corbel,[1] Julien Sage,[2] Jason H. Pomerantz,[1,3,*] and Helen M. Blau[1,*]
[1]Baxter Laboratory for Stem Cell Biology, Department of Microbiology & Immunology, Institute for Stem Cell Biology and Regenerative Medicine
[2]Departments of Pediatrics and Genetics
Stanford University School of Medicine, Stanford, CA 94305, USA
[3]Present address: Department of Surgery, Division of Plastic and Reconstructive Surgery, Program in Craniofacial and Mesenchymal Biology, Eli and Edythe Broad Center of Regeneration Medicine and Stem Cell Research, University of California, San Francisco, CA 94143, USA
*Correspondence: jason.pomerantz@ucsfmedctr.org (J.H.P.), hblau@stanford.edu (H.M.B.)
DOI 10.1016/j.stem.2010.05.022

SUMMARY

An outstanding biological question is why tissue regeneration in mammals is limited, whereas urodele amphibians and teleost fish regenerate major structures, largely by cell cycle reentry. Upon inactivation of *Rb*, proliferation of postmitotic urodele skeletal muscle is induced, whereas in mammalian muscle this mechanism does not exist. We postulated that a tumor suppressor present in mammals but absent in regenerative vertebrates, the *Ink4a* product ARF (alternative reading frame), is a regeneration suppressor. Concomitant inactivation of *Arf* and *Rb* led to mammalian muscle cell cycle reentry, loss of differentiation properties, and upregulation of cytokinetic machinery. Single postmitotic myocytes were isolated by laser micro-dissection-catapulting, and transient suppression of *Arf* and *Rb* yielded myoblast colonies that retained the ability to differentiate and fuse into myofibers upon transplantation in vivo. These results show that differentiation of mammalian cells is reversed by inactivation of *Arf* and *Rb* and support the hypothesis that *Arf* evolved at the expense of regeneration.

INTRODUCTION

Tissue regeneration in humans is extremely limited, which constitutes a major challenge to the repair of damaged organ and tissue function. Humans and other mammals do not regenerate large portions of lost muscles or other mesenchymal structures after traumatic injury or surgical excision. By contrast, some vertebrates such as the urodele amphibians and the teleost fish have a remarkable capacity to regenerate entire limbs, the lens of the eye, and portions of the heart (Poss et al., 2002; Brockes and Kumar, 2008; Tanaka and Weidinger, 2008). Although classically defined resident stem cells clearly play a role in tissue regeneration, their relatively low frequency in a given tissue may be insufficient to account for the massive regeneration observed in some lower vertebrates. In zebrafish, heart regeneration results from dedifferentiation and subsequent proliferation of cardiomyocytes (Poss et al., 2002). Substantial evidence from studies of newts and axolotls supports a similar regenerative mechanism, in which postmitotic limb tissues including muscles lose their differentiation markers, re-enter the cell cycle, proliferate, and then recapitulate differentiation in the blastema (Hay and Fischman, 1961; Lentz, 1969; Kintner and Brockes, 1984; Lo et al., 1993; Gardiner and Bryant, 1996; Echeverri et al., 2001). Recent observations strongly suggest that dedifferentiated cells of the limb remain lineage committed during this process (Kragl et al., 2009). In marked contrast, there is no evidence that dedifferentiation occurs as a natural part of tissue regeneration in mammals. This raises the possibility that a mechanism of regeneration involving reversal of differentiation of mesenchymal tissues, such as muscle, may have been lost or suppressed during evolution of higher vertebrates that, if elucidated, could significantly impact regenerative medicine.

Muscle differentiation in mammals occurs by a stepwise progression. This process entails morphological and functional changes driven by the expression of a series of muscle regulatory factors (MRFs), which induce expression of differentiation-specific genes such as creatine kinase and myosin heavy chain (MHC) (Molkentin and Olson, 1996). In particular, myogenin heralds a transition from proliferative myoblast to committed postmitotic muscle cell (Walsh and Perlman, 1997; Chargé and Rudnicki, 2004). Of critical importance to this transition is the expression of the retinoblastoma protein (pRb) (Gu et al., 1993; Lassar and Münsterberg, 1994; Novitch et al., 1996; Huh et al., 2004). The role of pRb in differentiation is multifaceted, including not only the orchestration of mitotic arrest and prevention of cell cycle reentry, but also inhibition of apoptosis and enforcement of stable tissue-specific gene expression (Burkhart and Sage, 2008). Because the differentiated state requires continuous active control (Blau et al., 1985; Blau and Baltimore, 1991; Yamanaka and Blau, 2010), ongoing expression of pRb or possibly redundant pocket proteins would be predicted to be necessary for the maintenance of the specialized muscle cell phenotype.

Attempts to reverse differentiation and postmitotic arrest in mammalian skeletal muscle cells by either acute suppression or permanent elimination of *Rb* have produced conflicting results. In newt muscle cells, cell cycle reentry and DNA

synthesis occur when pRb is inactivated by phosphorylation (Tanaka et al., 1997). Similarly, the inactivation of pRb by viral oncoproteins in immortalized mammalian myoblast cell lines, such as C2C12, readily results in BrdU incorporation and S phase reentry in nuclei of differentiated myotubes (Gu et al., 1993; Crescenzi et al., 1995), and is in agreement with more recent studies that use siRNA to suppress *Rb* (Blais et al., 2007). In marked contrast, in similar experiments with primary muscle cells isolated directly from mammalian muscle tissues, *Rb* reduction or elimination by Cre-mediated excision failed to result in significant S phase reentry (Sacco et al., 2003; Camarda et al., 2004; Huh et al., 2004). These data suggest that *Rb* loss in primary differentiated skeletal muscle cells is not sufficient to induce reversal of the postmitotic state in mammals, in stark contrast to the situation in urodeles.

We reasoned that components of the mammalian cell cycle machinery known to be absent in lower organisms could have evolved at the expense of regeneration. A prime candidate is the *Ink4a* locus, which encodes the structurally and functionally unrelated products p16ink4a and ARF (alternative reading frame). Both of these proteins are potent tumor suppressors that are frequently inactivated in human and mouse cancers. p16ink4a specifically inhibits cdk4 and functions upstream of *Rb*, whereas ARF binds MDM2, which results in p53 stabilization, in addition to having p53-independent functions (Sherr et al., 2005). Notably, ARF responds to oncogenic stimuli, including the inactivation of *Rb*, by inducing p53-dependent growth arrest or apoptosis (Sharpless and DePinho, 1999; Sherr et al., 2005). Although the *Rb* and *p53* pathways are evolutionarily ancient, their regulation by the *Ink4a* locus is a relatively new phenomenon. Homologs of *p16ink4a* exist in fish (Kazianis et al., 1999; Gilley and Fried, 2001). But the earliest identified *ARF* ancestor is in chickens, with no candidates in databases of lower organisms (Gilley and Fried, 2001; Kim et al., 2003; Brookes et al., 2004). Thus, the absence of *ARF* relatives could underlie certain fundamental differences in growth control in lower vertebrates.

Here we test the hypothesis that reversal of differentiation of mammalian skeletal muscle cells can be induced by inactivation of *Rb* in conjunction with *ARF*. Specifically, we postulated that upon loss of *Rb*, growth arrest and differentiation are maintained by induction of expression of the tumor suppressor *ARF*. Our data show that transient suppression of both *Rb* and *ARF* results in the ability of skeletal muscle cells to lose their differentiated properties, cycle, and then redifferentiate in a manner that mimics urodele cells. We used both genetic and biochemical approaches in primary cells and monitored single cell behavior by time-lapse microscopy, which enabled a rigorous analysis of the intrinsic control of muscle cell proliferation and modulation of the differentiated phenotype. The use of photoactivated laser microdissection (PALM) and laser pressure catapulting (LPC) to isolate single, morphologically intact, adherent, primary differentiated cells (myocytes) allowed the unambiguous identification of clones from individual cells. Based on our findings, we propose a molecular mechanism whereby evolution of *ARF* in part explains differences between urodele and mammalian skeletal muscle regeneration. The results suggest a means of replicating in mammals the robust regenerative response typical of urodeles, demonstrating that the *transient* induction of dedifferentiation could serve as an adjunct to classical tissue-specific stem cells.

RESULTS

Suppression of *Rb* by siRNA Induces S Phase Reentry in C2C12 Myotubes

The myoblast cell line C2C12 is a model system for studying muscle differentiation in vitro. In differentiation medium (DM), confluent C2C12 myoblasts exit the cell cycle and fuse with one another to form multinucleated muscle cells (myotubes), which express muscle proteins and are contractile. We developed a protocol to transiently express siRNAs in 66.8% of myotubes via the siImporter reagent (Figures S1A and S1B available online). To determine the duration and efficiency of siRNA treatment, C2C12 myotubes were treated with siRNAs against *Rb* (Rbsi) (Figures 1A and 1B). Semiquantitative RT-PCR and western analysis confirmed transient suppression of *Rb* transcript and protein levels (Figures 1B–1D). Treatment with Rbsi resulted in a decrease of pRb protein levels (Figure 1C) to approximately 50% ± 22% of the levels in control myotubes (Figure 1D). These data show that with siRNAs, pRb can be substantially reduced for a period of 48 hr.

To determine whether S phase reentry in C2C12 myotubes occurred after transient suppression of *Rb*, we labeled Mocksi- and Rbsi-treated myotubes with BrdU, as indicated in the scheme in Figure 1A. BrdU-labeled myonuclei were observed inside MHC^+ myotubes only after Rbsi treatment. S phase reentry was dependent on the dose of Rbsi used and doubled from 25.7% to 52.8% as the siRNA concentration was increased from 100 to 200 nM (Figure 1E). The 200 nm concentration was used in subsequent experiments. The percentage of myotubes that contained any BrdU-positive nuclei was analyzed in a separate set of experiments and found to be 25% (Figure S1H), which is explicable because myotubes with Brdu-positive nuclei often had large clusters of nuclei that underwent DNA synthesis, probably reflecting the successful transfection of a fraction of the cells in the culture (Figure S1A). Figure 1F shows representative images of BrdU incorporation together with MHC immunostaining to confirm differentiation. We found a marked change in myotube morphology 72 hr after transfection of Rbsi (Figure 1D, bottom) from a compact elongated structure with characteristic linear nuclear alignment to an amorphous structure, with nuclei aggregated in clusters, many of which were BrdU positive. These data confirm that transient suppression of *Rb* is sufficient to induce S phase reentry in differentiated C2C12 myotube nuclei and show that the extent of this effect depends on the concentration of Rbsi used.

Both *Rb* and *p19ARF* Must Be Suppressed for S Phase Reentry in Primary Myotubes

The majority of the data that suggest that suppressing *Rb* is sufficient for cell cycle reentry in mature mammalian myotubes comes from experiments with the C2C12 cell line (Gu et al., 1993; Velloso et al., 2001; Blais et al., 2007). Although useful for studying muscle cell differentiation and fusion (Pajcini et al., 2008), we reasoned that C2C12 cells, like other cell lines, may have acquired mutations essential to their immortalization. Therefore, we considered it critical to use primary cells to assess the role of pRb in maintaining the postmitotic state. We harvested primary myoblasts as previously described (Rando and Blau, 1994) from *Rosa26-CreER^{T2} Rb$^{lox/lox}$* mice (Viatour et al.,

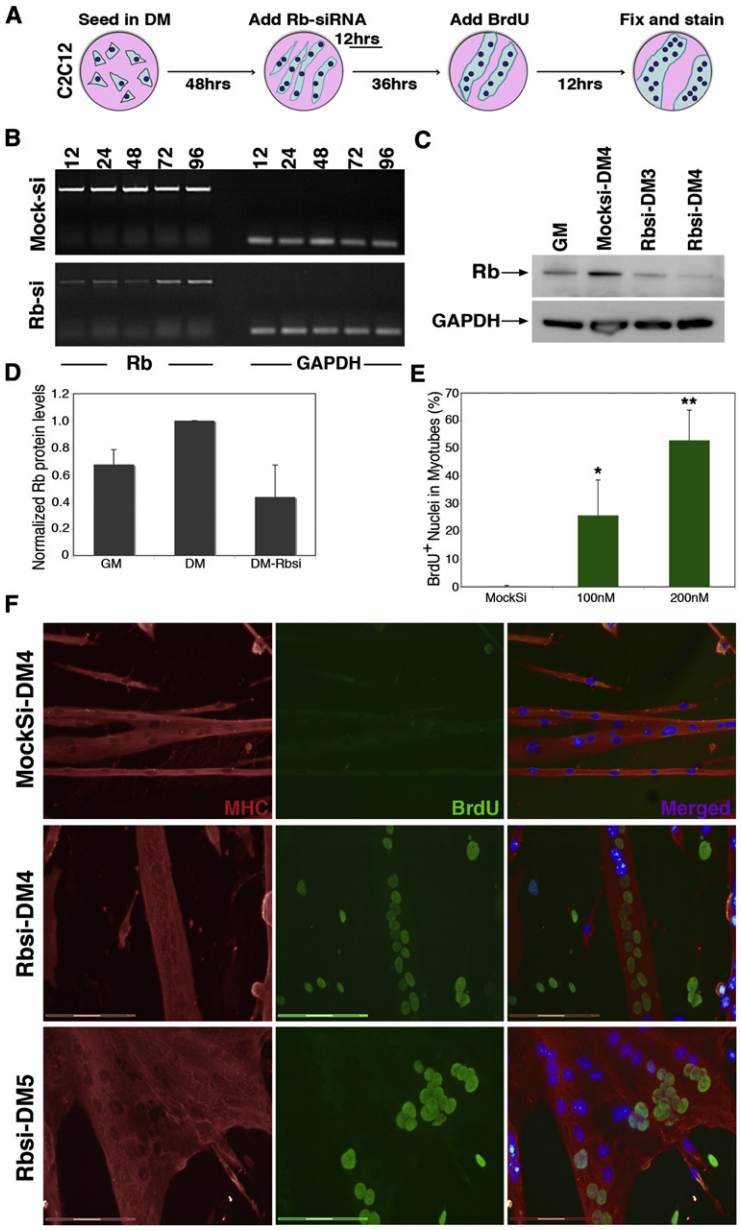

Figure 1. Suppression of Rb Is Sufficient for Cell Cycle Reentry in C2C12 Myotubes

(A) Schematic representation of the treatment of C2C12 myotubes.

(B) sqRT-PCR of *Rb* expression time course in hours after treatment with mocksi or Rbsi. GAPDH expression shown as RNA loading control.

(C) Western blot of protein expression levels of Rb (100 kDa) in C2C12 myoblasts (GM), myotubes (DM4), and myotubes at DM3 and DM4, 24 hr and 48 hr, respectively, after treatment with Rb-siRNA. GAPDH (35 kDa) as a loading control.

(D) Histogram representing the levels of Rb in GM, in DM4, and in DM4 treated with Rb-siRNA for 48 hr. Samples are normalized to Rb levels of DM4 myotubes.

(E) Histogram represents BrdU incorporation in myonuclei of myotubes in day 4 of differentiation (DM4), at least 36 hr after Rbsi treatment. A minimum of 500 nuclei were counted from random fields for each trial.

(F) Immunofluorescence images from mock-treated DM4 C2C12 myotubes and 200 nM Rbsi-treated myotubes in DM4 and DM5. Myotubes were labeled with primary antibody for MHC (red) and BrdU (green), as well as with Hoechst 33258 dye (blue). Scale bars represents 150 μm. Growth medium (GM); myotubes cultured in differentiation medium for 4 or 5 days (DM4 or DM5, respectively).

Error bars indicate the mean ± SE of at least three independent experiments, p value was determined with a t test (*$p < 0.05$, **$p < 0.01$).

2008) crossed to mice carrying a Cre-responsive β-galactosidase reporter allele (Soriano, 1999). In these mice, Cre expression and *Rb* excision is dependent on tamoxifen (TAM) induction (Figures S1C and S1D). In primary myotube cultures, a single 24 hr treatment with 1 μM TAM was sufficient to reduce *Rb* expression (Figure S1E). Both transcript and protein levels dropped substantially by 96 hr after TAM treatment (Figure 2C; Figure S1F).

We analyzed S phase reentry in primary myotubes after loss of *Rb* expression according to the scheme in Figure 2A. In contrast to C2C12 myotubes, in primary myotubes regardless of whether *Rb* was knocked down by Rbsi (Figure 2B) or excised by Cre expression (Figure 2D, top), in more than 1500 nuclei scored from random fields of MHC^+ myotubes, BrdU labeling of myonuclei was relatively rare (Figure 2G). In the representative images in Figures 2B and 2D, $BrdU^+$ nuclei are detectable, but these are generally not within MHC^+ myotubes. Thus, loss of *Rb* in primary myotubes is not sufficient to induce cell cycle reentry.

We observed that acute suppression of *Rb* in primary myotubes led to upregulation of *p19ARF* mRNA (Figure S1F) and protein (Figure 2C, third lane). These results are in agreement with previous reports showing that disruption of *Rb* function by mutation or by hyperphosphorylation in response to mitogenic signals leads to the activation of *ARF* (DeGregori et al., 1997; Sage et al., 2003). ARF, in turn, serves to block inappropriate cycling. Induction of *ARF* was accompanied by a mild increase in baseline levels of apoptosis, but the majority of myotubes remained robust and viable. Apoptosis was rarely observed in siRNA-treated cells in which p16/p19 was reduced (Figure S1I).

In contrast to primary cells, *p19ARF* was not detected in C2C12 myotubes in response to *Rb* suppression (Figure 2E). We determined by genomic PCR analysis that the lack of *p19ARF* expression in C2C12 cells was due to a deletion in the *Ink4a* locus (Figure 2F), a characteristic of murine cell lines immortalized by continuous passage in culture (Sherr and DePinho, 2000). These observations suggested that the disparate cell cycle reentry responses of primary and immortalized muscle cells to loss of *Rb* might be related to the status of ARF. To test whether the suppression of the *Ink4a* gene products in *Rb*-deficient primary myotubes would permit reentry, we designed siRNAs that target the shared exon 2 region of *Ink4a* mRNA (p16/19si), the ARF-specific exon 1β (p19ARFsi), and

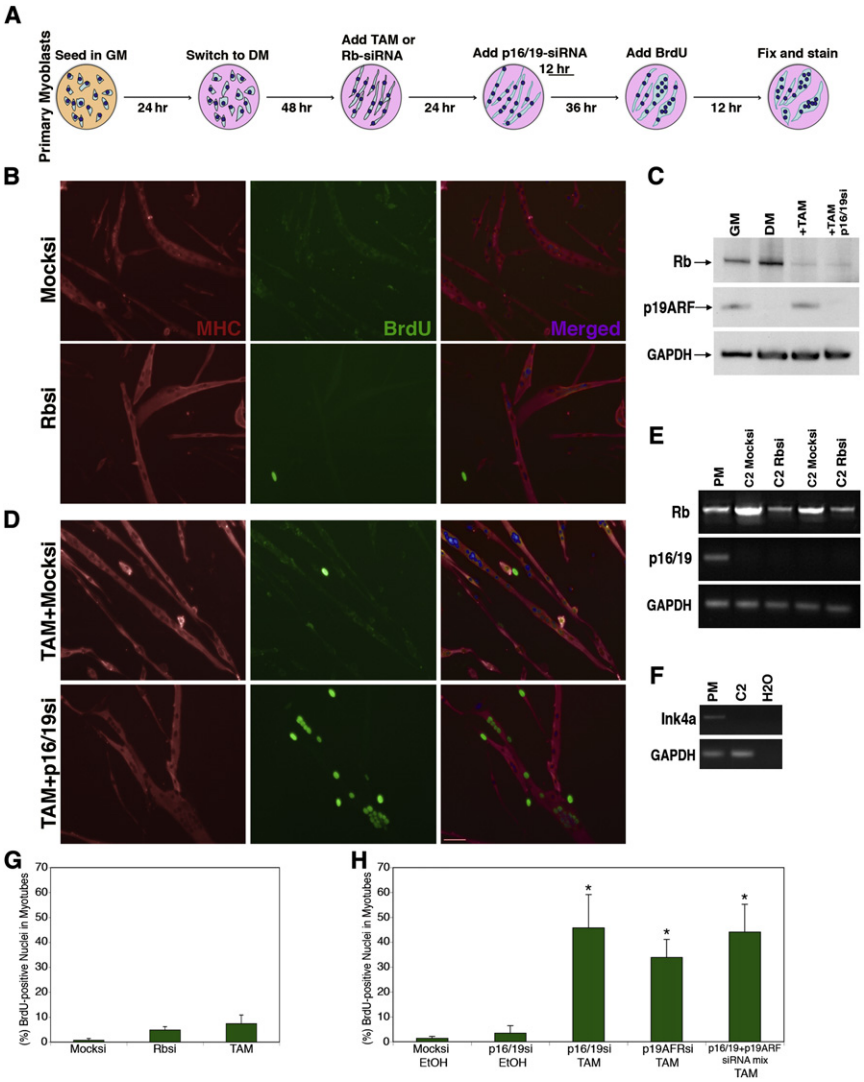

Figure 2. Suppression of *Rb* and *p16/19* Is Necessary for Cell Cycle Reentry in Primary Myotubes

(A) Schematic representation of the treatment of primary myotubes with either tamoxifen (TAM) and/or siRNA.

(B) Immunofluorescence images from mock si-Glo-treated primary myotubes and Rbsi-treated myotubes. Myotubes were labeled with primary antibody for MHC (red) and BrdU (green), as well as with Hoechst 33258 dye (blue). Scale bar represents 50 μm.

(C) Western blot of primary myotube protein levels; Rb (100 kDa) and p19ARF (20 kDa) in GM and DM5, after TAM treatment or TAM and p16/19si treatment. GAPDH (35 kDa) as loading control.

(D) Immunofluorescence images indicating BrdU incorporation in TAM- and mock si-Glo-treated primary myotubes compared to TAM- and p16/19si-RNA-treated primary myotubes.

(E) sqRT-PCR showing Rb and *Ink4a* (*p16/19*) expression in primary myotubes as well as in two different C2C12 myotube populations treated with Mocksi or Rbsi.

(F) sq-PCR amplification with primers for the shared exon 2-3 region of the *ink4a* locus, from genomic DNA prepared from primary myoblasts and C2C12 myoblasts.

(G) Histogram represents BrdU incorporation in primary myotube nuclei at DM5, after suppression of Rb with either siRNA or TAM.

(H) Histogram represents BrdU incorporation in primary myotube nuclei after treatment with TAM and siRNAs against *ink4a* gene products. A minimum of 500 nuclei were counted from random fields for each trial in (G) and (H).

Error bars indicate the mean ± SE of at least three independent experiments. *$p < 0.01$.

the p16-specific exon 1α. Primary myotubes were first treated with TAM or Rbsi, then 24 hr later transfected either with p16si, p16/19si, p19ARFsi alone, or both p16/19si and p19ARFsi together (see scheme in Figure 2A). Gene knockdown in myotubes was verified by western analysis (Figure 2C) and by RT-PCR (Figure S1G). When labeled with BrdU after TAM and p16/19si treatment, differentiated myonuclei incorporated BrdU in MHC-positive myotubes (Figure 2D). Quantification of the BrdU labeling indicated that 45.7% ± 7.2% of myonuclei enter S phase in TAM- and p16/19si-treated myotubes, a marked increase over baseline values observed in myotubes treated only with TAM or p16/19si (Figures 2G and 2H). Different combinations of siRNAs that exclusively induced knockdown of *p19ARF* or that targeted both *Ink4a* gene products in TAM-treated cells yielded similar results (Figure 2H). Notably knockdown of p16 alone after TAM treatment did not increase BrdU incorporation above background levels (data not shown), suggesting that ARF was primarily responsible for the observed *Ink4a* effects. Therefore, for subsequent experiments we used the p16/19si (exon 2) because it produced the strongest suppression of *p19ARF*. Thus, robust S phase reentry in differentiated primary mammalian myotubes occurs only after combined suppression of both *Rb* and *p19ARF*.

Upregulation of Mitotic and Cytokinetic Components in *Rb*- and *p16/19*-Deficient Myonuclei

To determine whether S phase reentry in primary myonuclei marked the initiation of the mitotic process, we analyzed control or TAM- and p16/19si-treated nuclei for the induction of expression of a panel of mitotic and cytokinetic proteins. AuroraB and survivin are components of the chromosome passenger complex (CPC), which controls spindle structure, kinetochore attachment, and chromosome segregation (Ruchaud et al., 2007). Anillin is important in the organization of the cleavage furrow during cytokinesis (Hickson and O'Farrell, 2008). In addition, we characterized expression of cyclins D1 and E as well as Emi1/FBXO5, which regulates progression through early mitosis by preventing premature activation of APC (Reimann et al., 2001). We analyzed mitotic progression by investigating the localization of Eg5, a motor protein in the kinesin-like family

involved in spindle dynamics during mitosis (Sawin and Mitchison, 1995).

Anillin and each of the CPC components described above are expressed in primary proliferating myoblasts, but their mRNA and protein levels drop precipitously once myotubes form (Figures S2A and S2B). When Rb was excised in differentiated primary multinucleated myotubes after TAM treatment, *anillin*, *AuroraB*, and *survivin* mRNA levels all rose, despite high levels of *p19ARF* expression (Figure S2A). However, protein levels of AuroraB and survivin were comparable to those of growing myoblasts only after concomitant suppression of *Rb* and *p19ARF* (Figure S2B). To verify that upregulation of CPC components occurred specifically in myonuclei that had entered S phase, primary myoblasts were labeled with BrdU for 12 hr then stained for BrdU and survivin. Dividing primary myoblasts were positive for both BrdU and survivin, with the latter marking the cleavage furrow (data not shown). Differentiated, control-treated myotubes did not have myonuclei that expressed survivin, but those treated with TAM and p16/19si exhibited clustered $BrdU^+$ myonuclei, and in these same myonuclei survivin expression was upregulated (Figure S2C, bottom). Although survivin was not localized in organized cleavage furrows, quantification of the immunostaining results indicated that nearly 80% of the myonuclei that had re-entered S phase also upregulated survivin (Figure S2D).

Analysis of the expression of cyclins D and E1 showed that these gene products are expressed in proliferating myoblasts and downregulated in differentiated myotubes. Upon treatment with either TAM or with TAM and p16/19si together, there was a rise in the expression of these cyclins as well as Emi1/FBXO5 (Figure S2E). These data indicate that mature myonuclei in myotubes progress through S phase. In order to determine the extent of mitotic progression, we analyzed Eg5 localization in myotubes treated with TAM and p16/19si. Our results indicate that despite upregulation of Eg5, bipolar spindles did not form in *Rb*- and *p16/19*-deficient myotubes, although monopolar clustering of Eg5 was frequently observed (Figure S2F). Full karyokinesis or cytokinesis was not observed in myotubes.

Taken together, our data suggest that primary multinucleated myotubes deficient in both pRb and ARF synthesize DNA and components of the mitotic machinery, but fail to assemble these proteins in a manner required for nuclear division. Whereas the incorporation of BrdU and expression of Ki67 mark the occurrence of S phase, Aurora B is maximally expressed in G2-M. Moreover, survivin is synthesized in G2-M only in accordance with the cell cycle-dependent CDE/CHR boxes in its promoter and posttranslational stabilization that occurs at this cell cycle phase (Kobayashi et al., 1999; Li and Altieri, 1999). However, the diffuse pattern of survivin immunostaining (Figure S2C) indicates that the nuclei in dedifferentiating mytotubes did not enter prophase, during which survivin staining becomes punctate (Caldas et al., 2005). Furthermore, Eg5, although upregulated at the protein level, does not form the typical pericentrosomal clustering signifying the onset of prophase (Sawin and Mitchison, 1995). Thus, our data indicate that suppression of pRb and ARF in intact myotubes results in progression through S phase to G2, but the nuclei cannot complete M phase and are arrested at the onset of mitosis.

Dedifferentiation Accompanies S Phase Reentry in Primary Muscle Cells

Postmitotic differentiated muscle cells express phenotypic markers such as myosin heavy chain (MHC) and a characteristic elongated morphology that results, in part, from the arrangement of the microtubule network. During differentiation, the microtubule cytoskeleton shifts from the radial, centrosomal arrangement typical of myoblasts and most mononucleated mitotic cells to a noncentrosomal array that extends along the longitudinal axis of the multinucleated myotube (Bartolini and Gundersen, 2006). We investigated the role of the *Rb* and *Ink4a* gene products in sustaining expression of the differentiated phenotype by analyzing morphology and expression of markers of differentiation. Immunostaining demonstrated that MHC is not expressed in proliferating myoblasts or during early differentiation, but is readily detectable in all nascent myotubes by day 4 in differentiation media (Figure 3A, top). Treatment with tamoxifen after differentiation did not significantly alter myotube morphology and did not result in a detectable change in MHC levels by immunostaining (Figure 3A, bottom right). However, combined deletion of *Rb* and suppression of *ink4a* caused a marked decrease in MHC expression in cultures that had previously been differentiated (Figure 3A, bottom). Although intact, multinucleated and viable myotubes were present at days 6 and 7 of differentiation, cells that were rendered deficient in *Rb* and *ink4a* products lost structural integrity and began to collapse by day 6. By day 7, primary myotube morphology and MHC levels had severely deteriorated when compared to myotubes treated only with TAM and mock siRNAs (Figure 3A, bottom).

The combined suppression of *Rb* and *p16/19* resulted in a decrease in levels of differentiation-specific muscle proteins in addition to MHC. *Rb* loss alone in primary myotubes treated with TAM led to a moderate reduction in some myogenic protein levels, such as MHC and myogenin (Figures 3B, 3C, and 3F) and a moderate increase in the mitotic proteins AuroraB and survivin (Figure 3B). However, suppression of both *Rb* and *p19ARF* was more profound and accompanied by substantially reduced levels of myogenin and M-CK in addition to MHC (Figure 3F; Figure S3D, upper band). In agreement with findings in primary myotubes in which both Rb and p19/ARF proteins were absent, western blot analyses of C2C12 myotubes, which already lack *p19ARF*, exhibited decreased MHC levels when treated only with Rbsi (Figure S3A). Expression levels of *MRF4* also declined. Semiquantitative RT-PCR analyses revealed a decrease in RNA levels that paralleled these protein data (Figure S3C).

Immunofluorescence (IF) analysis of myotubes revealed several morphological differences in TAM and p16/19si myotubes when compared to Mocksi myotubes. In addition to incorporating BrdU by day 6 of differentiation, treated myotubes were significantly less compact than controls, never exhibited striations, and appeared to have large gaps in their MHC network (Figure 3D). Whereas mock-treated primary myotubes retained their elongated morphology and nuclear organization, $BrdU^+$ myotubes collapsed into amorphous multinucleated syncytial structures, highlighted by the clustering of myonuclei. Although not all of the myonuclei entered S phase, loss of structural integrity of the myotube is probably due to the lack of maintenance of myotube nuclear protein domains. Morphological

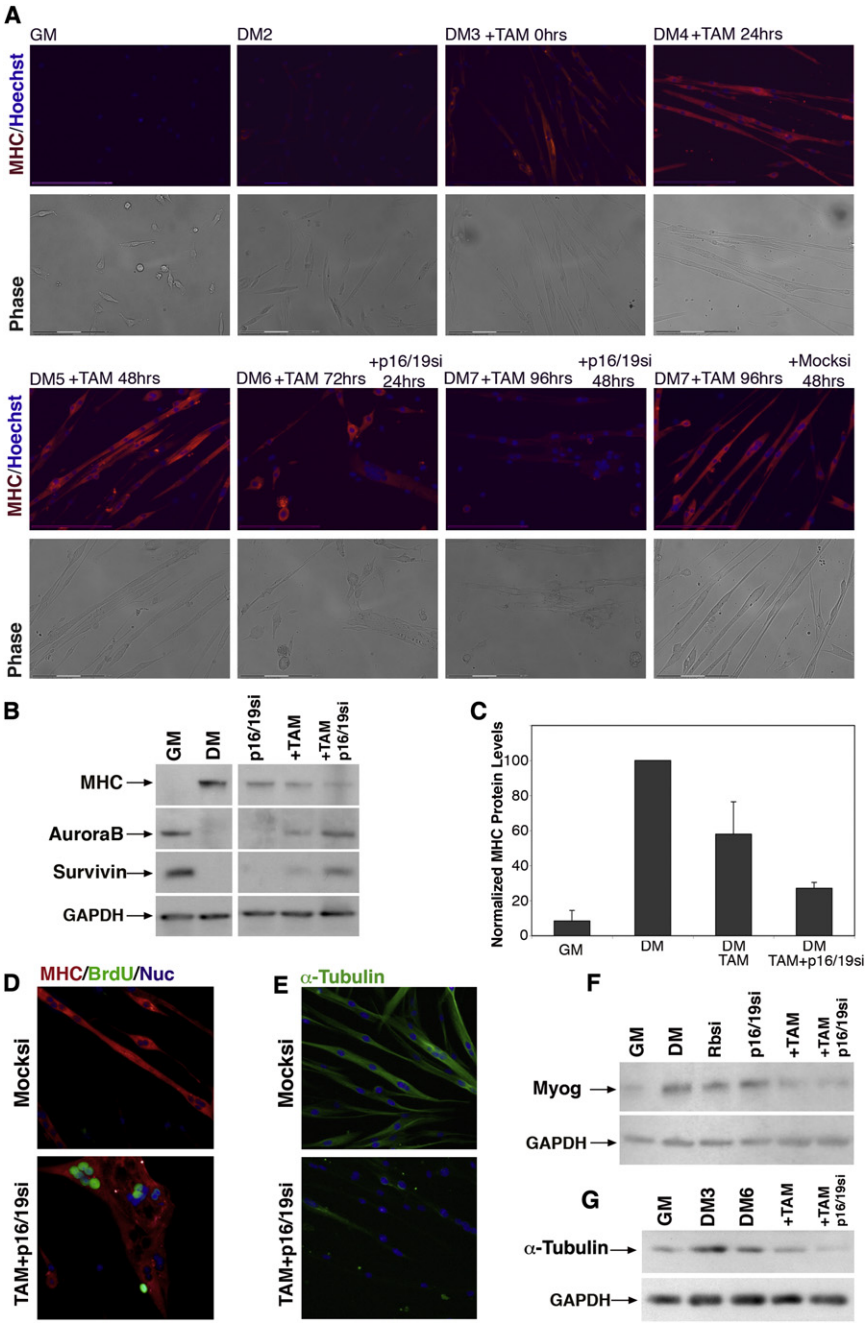

Figure 3. Dedifferentiation of Mature Myotubes

(A) Immunofluorescence images of primary myoblasts and myotubes cultured for indicated times in DM and treated with TAM and either nonspecific siRNA (Mocksi) or p16/19si at the indicated time points. Myotubes were labeled with primary antibodies for MHC (red) and Hoechst 33258 (blue). Bottom panels: phase images of the same image fields. Scale bars represent 150 μm.

(B) Western blot analysis of primary myoblasts in GM and DM5 showing expression of MHC (220 kDa), AuroraB (38 kDa), and Survivin (20 kDa) as well as expression of these same proteins in myotubes after treatment for at least 48 hr with siRNA against p16/19, with TAM or both TAM and p16/19si.

(C) MHC protein levels normalized to differentiated myotube cultures. Primary myotubes were treated with TAM or TAM and p16/19si. Growth medium (GM), differentiation medium (DM). Error bars indicate the mean ± SE of at least three independent experiments.

(D) Representative immunofluorescence images of DM6 primary myotubes treated with EtOH and nonspecific siRNA or TAM and p16/19si for at least 48 hr. Myotubes were labeled with primary antibodies for MHC (red), BrdU (green), and Hoechst 33258 (blue).

(E) Representative immunofluorescence images of primary DM6 myotubes after Mocksi or TAM and p16/19si treatment. Myotubes were labeled with primary antibodies for α-tubulin (green) and Hoechst 33258 (blue).

(F and G) Western blot analysis of Myogenin (36 kDa) (F) and α-tubulin (50 kDa) (G) in primary myoblasts and myotubes treated as indicated with siRNA and/or TAM. In each of the blots, GAPDH (35 kDa) is the loading control. Growth medium (GM); myotubes were cultured in differentiation medium for 3 or 6 days (DM3 or DM6, respectively).

changes and loss of MHC expression were also correlated with BrdU$^+$ staining in C2C12 myotubes; however, only loss of pRb was required (Figure S3B).

To further investigate the deterioration in myotube morphology, we analyzed the expression and arrangement of α-tubulin in mature myotubes. In mock-treated myotubes, α-tubulin is expressed at high levels and microtubules are arranged longitudinally, whereas in TAM- and p16/19si-treated myotubes, α-tubulin levels are lower by IF (Figure 3E) and western analysis (Figure 3G; Figures S3E and S3F). To dynamically visualize structural deterioration, myotubes were imaged by time-lapse microscopy after treatment with TAM and Mocksi (Movie S1) or TAM and p16/19si (Movie S2). A time-lapse comparison shows that complete morphological collapse of myotube structure takes place only after loss of both the *Rb* as well as *Ink4a* gene products. Despite extensive structural differences, the *Rb*- and *ink4a*-deficient primary myotubes do not die or detach faster than Mocksi-treated myotubes, and they retain their motility and membrane activity, such as filopodia and lamellapodia.

Terminally Differentiated Myocytes Are Capable of Proliferation after Suppression of *Rb* and *p16/19*

The extent of muscle differentiation can be characterized based on the sequential expression of muscle regulatory transcription factors (MRFs). MyoD and Myf5 are early and characteristic of cycling myoblasts, whereas late transcription factors include myogenin and MRF4, which are expressed in terminally

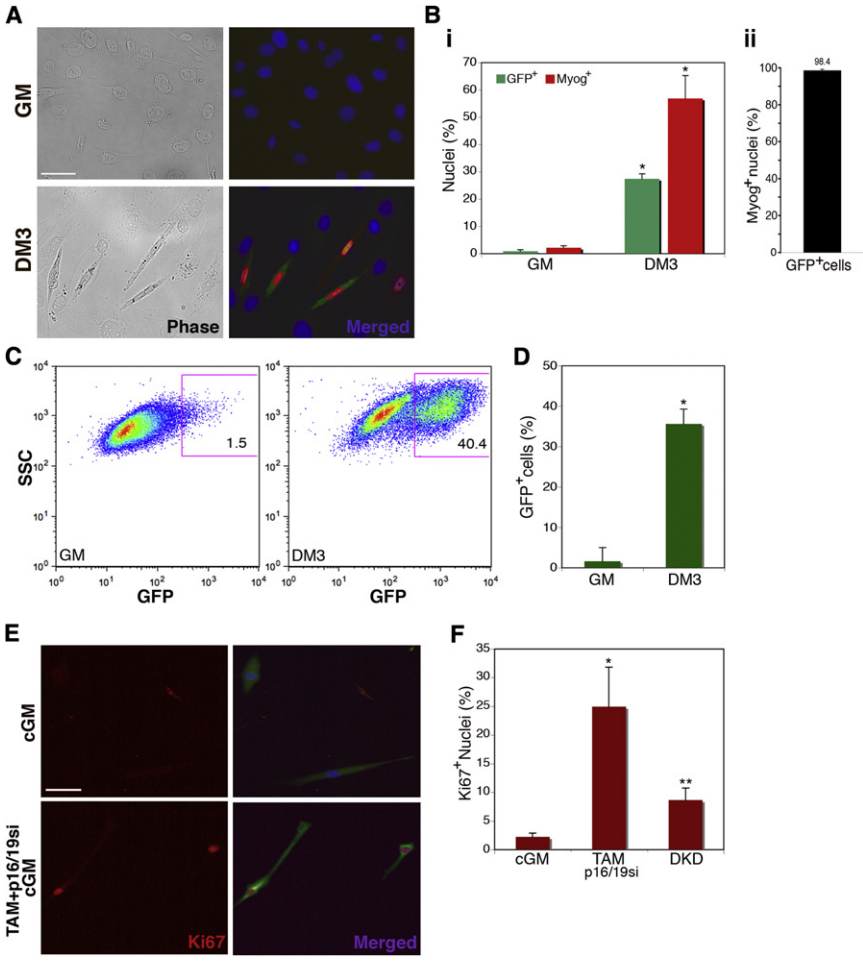

Figure 4. Myogenin-Expressing Myocytes Enter S Phase Only after Loss of *Rb* and *ink4a* Gene Products

(A) Immunofluorescence images of myoblasts (GM) and myocytes (DM3) infected with pLE-myog3R-GFP. Cells were labeled with primary antibodies for GFP (green), myogenin (red), and Hoechst 33258 (blue). Scale bar represents 50 μm.

(B) (i) Histogram represents percentage of GFP-positive (green bars) and myogenin-positive (red bars) cells in growth medium (GM) or differentiation medium (DM3). A minimum of 1000 nuclei were counted from random fields for each trial. Error bars indicate the mean ± SE of at least three independent experiments (*$p < 0.005$). (ii) Histogram represents percentage of GFP-positive cells that also express detectable myogenin by immunostaining. Individual cells were evaluated for expression of each marker. A minimum of 250 cells were counted from random fields. Error bars indicate the mean ± SE of three independent experiments.

(C) Representative FACS plots of myoblasts (GM) and myocytes (DM3) infected with retroviral pLE-myog3R-GFP construct. Gated population indicates GFP-positive myocyte population employed in subsequent experiments.

(D) Histogram representation of GFP expression in three independent experimental FACS profiles on myoblasts (GM) and myocytes (DM3) (*$p < 0.001$).

(E) Immunofluorescence images of GFP-positive FACS-sorted myocytes cultured in conditioned GM only (cGM) or in cGM with TAM and p16/19si-RNA. Cells were labeled for Ki67 (red) and GFP (green) as well as Hoechst 33258 (blue). Scale bar represents 50 μm.

(F) Histogram represents percent of Ki67-positive nuclei in GFP-positive FACS sorted population, in cGM, treated with TAM and p16/19si, or treated with Rbsi and p16/19si-RNA in tandem (DKD). Growth medium (GM); a minimum of 100 nuclei were counted from random fields for each trial. Error bars indicate the mean ± SE of three independent experiments (*$p < 0.01$, **$p < 0.005$).

differentiated myocytes and myotubes (Shen et al., 2003; Chargé and Rudnicki, 2004). Based on this pattern of transcription, we developed a system to study cycling and dedifferentiation in prospectively isolated populations derived from individual differentiated muscle cells. We infected low-passage *Rosa26-CreER^{T2} Rb$^{lox/lox}$* primary myoblasts with a retroviral vector in which GFP expression is under the control of the *myogenin* promoter (pLE-myog3R-GFP). To verify the fidelity of *myogenin* and *GFP* coexpression, pLE-myog3R-GFP myoblasts were sparsely seeded in growth medium or differentiation medium for 72 hr and stained for myogenin and GFP. IF analysis clearly showed that GFP and myogenin expression were upregulated in the differentiating (DM3) myocyte population (Figure 4A). Quantification of IF data indicated that only 0.9% of the cells are GFP positive in growth conditions, probably representing spontaneous differentiation. In differentiated cultures, GFP expression correlated with myogenin immunoreactivity, and 27% ± 2.0% of the cells had detectable GFP levels (Figure 4Bi). To verify the fidelity of myogenin expression in GFP-positive cells, we scored elongated GFP-positive myocytes for myogenin. Our data indicate that 98.4% ± 1.8% of cells were GFP$^+$ myogenin$^+$ (Figure 4Bii). High-throughput analysis of GFP expression in myoblasts and myocytes was also performed by fluorescence activated cell sorting (FACS), which showed that 35% of the cells expressed GFP after 3 days in differentiation medium, whereas only 1.8% of cells in growth medium were GFP$^+$ (Figure 4D). Thus, pLE-myog3R-GFP infection of primary myoblasts allows for reliable identification of myogenin-expressing cells.

Myoblasts seeded at low-density express *myogenin* and undergo terminal differentiation in the absence of fusion (Shen et al., 2003). We took advantage of this in vitro property of muscle cells to investigate whether the dedifferentiation and cell cycle reentry observed in differentiated multinucleated myotubes could lead to proliferation after suppression of *Rb* and *p19ARF* in differentiated mononucleated myocytes. In order to follow the fate of single cells, the following experiments were performed with individual pLE-myog3R-GFP myocytes. First, sparsely seeded primary muscle cells, maintained in DM for 72 hr, were sorted on the basis of GFP expression as depicted

by the gated population in Figure 4C. To determine whether the differentiated muscle cells were capable of proliferation, the FACS-sorted population was cultured in conditioned growth medium (cGM) for up to 48 hr and then stained for GFP and Ki67 (Figure 4E, top). Only 2.3% of GFP$^+$ cells had Ki67-positive nuclei. In contrast, GFP$^+$ cells treated with TAM 24 hr prior to FACS sorting and with p16/19si 12 hr after FACS sorting (Figure 4E, bottom) exhibited Ki67 nuclear staining in 25% of the GFP$^+$ population 48 hr after culture in cGM (Figure 4F).

As an alternative method to suppress *Rb* and *p16/19*, siRNAs against *Rb* and *p16/19* were used to transiently reduce both transcripts. Analyses to determine the ideal dosage and method of siRNA application showed that most efficient double knockdown (DKD) occurred after tandem treatment of primary muscle cells with Rbsi, a 12 hr recovery period, followed by treatment with p16/19si. DKD treatment of FACS-sorted GFP$^+$ cells resulted in 8.6% Ki67$^+$ nuclei (Figure 4F). That the frequency of DNA synthesis was lower in DKD-treated cells than in those treated with TAM and p16/19si was expected given the lower efficiency of knockdown compared to TAM treatment for *Rb* suppression. The data from these two types of experiments show that at the single cell level, differentiated *myogenin*-expressing myocytes, like myotubes, efficiently enter S phase only after suppression of both *Rb* and *Ink4a* gene expression.

We reasoned that if myocytes could divide, they would give rise to clones. However, to rule out cell migration and definitively show that a postmitotic myocyte divided, single-cell resolution and clonal analysis was critical. Accordingly, to assess the proliferative potential of myocytes, we first FACS-purified cells twice in order to isolate individual differentiated GFP$^+$ myocytes. Individual myocytes were then sorted directly into microarrays of hydrogel wells (Figure S4A; Lutolf et al., 2009), while a subset was stained for coexpression of GFP and myogenin (Figure S4B). After treatment with Mocksi or DKD, proliferative myocytes were scored as the percentage of microwells that had a minimum of 8 cells at 96 hr after treatment. 6.8% of DKD-treated myocytes gave rise to clones in contrast to only 0.6% of Mocksi-treated cells (Figure S4C). Taken together, these data support the conclusion that myogenin-positive myocytes acquire proliferation potential after suppression of *Rb* and *p16/19* expression.

Clonal Expansion and Proliferation of Individually Purified Myocytes after Laser Microdissection and Laser Pressure Catapulting

To determine definitively whether differentiated myocytes dedifferentiate and proliferate, it is essential to monitor individual myocytes before and after loss of pRb and ARF. For this purpose we pioneered the use of photoactivated laser microdissection (PALM) and laser pressure catapulting (LPC) with primary cells. LPC is extensively used to obtain precise regions of fixed tissues for DNA, RNA, and protein analyses. However, the use of LPC for studies of living cells has been reported only in methodological descriptions with robust cell lines in protocols by the developers of PALM (Stich et al., 2003; Schutze et al., 2007). We optimized LPC in order to ensure cell viability and isolate single cells from mass cultures of primary myoblasts and myocytes. With the PALM LPC system, cells are selected for isolation by the operator, who encircles the cell of interest with a unique software-simulated shape; then the laser is directed to cut the membrane precisely along the operator-drawn lines. The cut membrane is subsequently catapulted by laser pressure and captured by a robotic arm carrying an inverted media-containing cap. During this procedure, the captured cell remains attached to the membrane on which it grew, so that cell adhesion and morphology are not disrupted. This technology allows a single cell to be isolated intact on the surface on which it is growing. Via LPC, the identification of a clone derived from a captured cell is unambiguous because it is plated singly in a well. In this way there is no question regarding the origin of the cells that proliferate.

Laser microdissection and pressure catapulting analysis was performed with myocytes. For this purpose primary myoblasts expressing pLE-myog3R-GFP$^+$ were sparsely seeded and differentiated to become GFP$^+$ myocytes and then treated with either mock siRNA (Figure 5A) or for suppression of *Rb* and *ARF* (Figures 5Bi and 5Ci). Individual myocytes were selected based on their differentiated phenotype including elongated morphology evident by phase microscopy (Figure 5Ai, left) and bright GFP expression (Figures 5Bii and 5Cii, left). Laser microdissection was used to mark and cut the membrane surrounding prospectively identified single myocytes (green lines Figures 5Bii and Figure 5Cii). Marking and recording membrane shapes allowed for tracking of each membrane and the isolated cell on its surface. The LPC burst locations that lead to catapulting are indicated by the blue dots in the images in Figure 5Bii, which also serve as a means of identifying the membrane. Typical images obtained during the steps of the PALM and LPC isolation process are shown in Figures 5Bii and 5Cii. Myocyte morphology before and after membrane ablation did not significantly change. Note in the example shown that 72 hr after capture, the mock-treated myocyte is still associated with the membrane (Figure 5Aii, panel 4), and by 96 hr it has left the membrane but still exists as a single adherent cell, although it was cultured in conditioned growth medium since the time of capture (Figure 5Aii, panel 5). Similarly, in individual myocytes treated for reduction of *Rb* and *ARF*, morphology remained intact during the cutting and catapulting (Figures 5Bii and 5Cii, left 3 panels). However, in contrast to mock-treated myocytes, reduction of *Rb* (TAM or siRNA) and *ARF* (siRNA) led to cell division and colony formation in the immediate vicinity of the membrane (Figure 5Bii, fourth panel from left, Figure 5Cii, fourth panel from left). Additional examples of single GFP$^+$ myocyte laser capture are shown in Figures S4D and S4E.

In five independent PALM LPC isolation experiments, an analysis of a total of 250 membranes verified that without reduction of *Rb* and *ARF*, not a single captured myogenin-GFP$^+$ myocyte divided to produce a colony. In contrast, deletion of *Rb* and suppression of *ARF* produced 34 colonies, a frequency of 13.8% (Figure 5D), and transient suppression of both *Rb* and *ARF* (DKD) resulted in a colony frequency of 8.0%.

To increase the efficiency of identification of single GFP$^+$ myocytes, and to thereby avoid desiccation, we increased viability by first using FACS to enrich for myocytes expressing myogenin-GFP, thus facilitating identification of single myocytes (Figure S5A). Images of the captured control or TAM- and p16/19si-treated myocytes are shown (Figures S5B and S5C). Again, control-treated myocytes failed to produce colonies in conditioned growth medium (Figure S5B), whereas myocytes in which

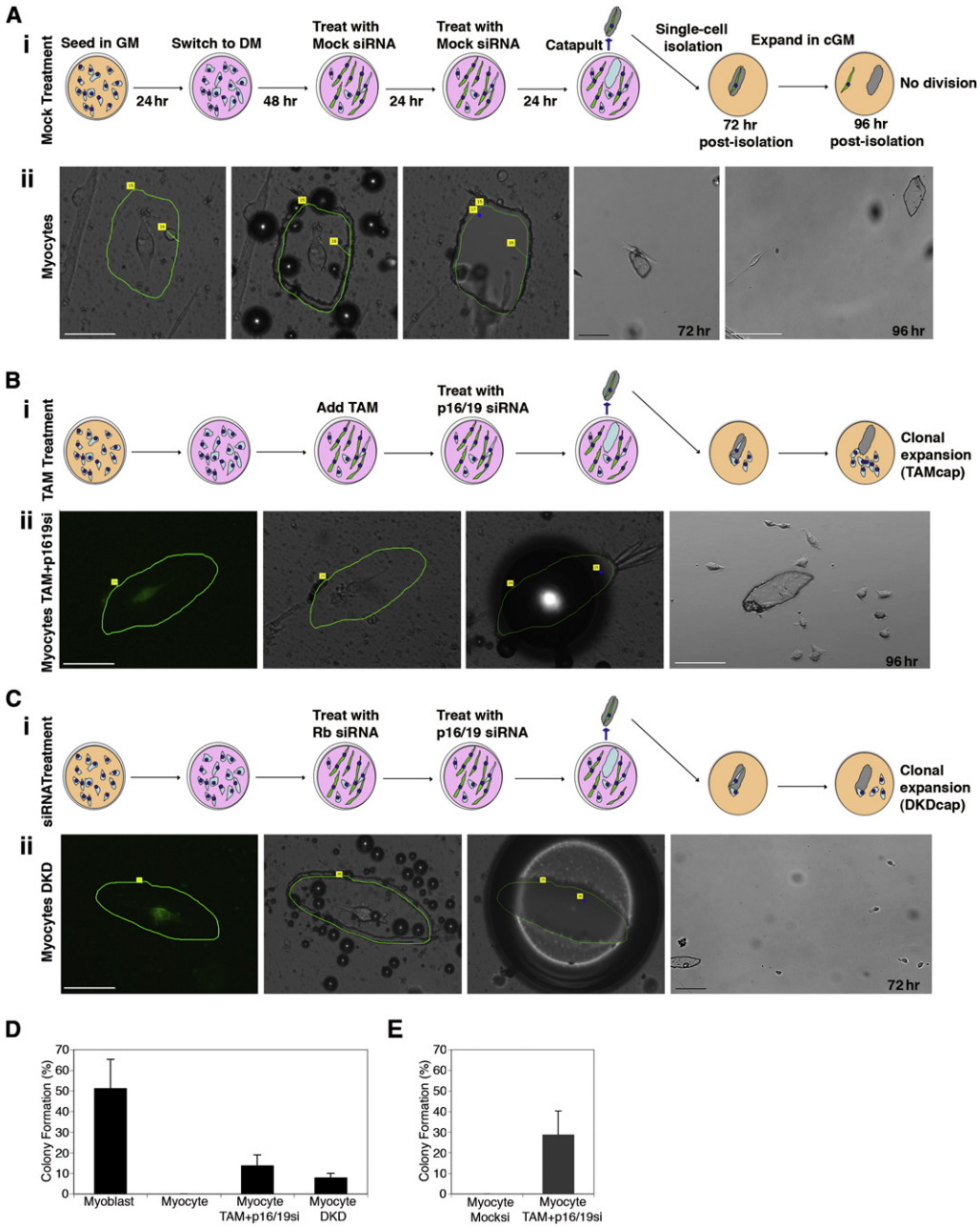

Figure 5. Laser Microdissection and PALM LPC; Single Cell Isolation and Clonal Expansion of Dedifferentiated Myocytes

(A) (i) Schematic representations of the culture conditions, treatment with mock siRNA, and isolation by laser microdissection and catapulting of myogenin-GFP$^+$ myocytes. Diagram also shows the fate of isolated cells 72 and 96 hr after isolation. (ii) Representative images of mock-treated myocyte (DM4) (panels left to right) prior to microdissection, immediately after microdissection, after LPC isolation, 72 hr postisolation, and 96 hr postisolation. Scale bars represent 50 μm and 100 μm.

(B) (i) Schematic representations of the culture conditions, treatment with TAM and p16/19 siRNA, and isolation by laser microdissection and catapulting of myogenin-GFP$^+$ myocytes. Diagram also shows the fate of isolated cells 72 and 96 hr after isolation. (ii) Representative image of TAM- and p16/19siRNA-treated myocyte (DM4): First panel, native GFP expression marks myogenin expression prior to microdissection; second panel, the same cell during microdissection; third panel, after LPC isolation; fourth panel, 96 hr postisolation and visualization of expansion. Scale bars represent 50 μm and 100 μm.

(C) (i) Schematic representations of the culture conditions, treatment with Rb and p16/19 siRNA, and isolation by laser microdissection and catapulting of myogenin-GFP$^+$ myocytes. Diagram also shows the fate of isolated cells 72 and 96 hr after isolation. (ii) Representative image of DKD-treated myocyte: first panel, GFP expression marks myogenin expression prior to microdissection; second panel, the same cell after microdissection; third panel, after LPC; fourth panel, 72 hr postisolation with visualization of expansion. Scale bars represent 50 μm and 200 μm.

(D) Histogram represents percentage of colony formation after PALM LPC cell isolation. Error bars indicate the mean ± SE of at least five independent experiments, in which at least 50 membranes were captured for each myocyte trial, and at least 20 myoblast membranes were captured to verify cell survival and capture efficiency.

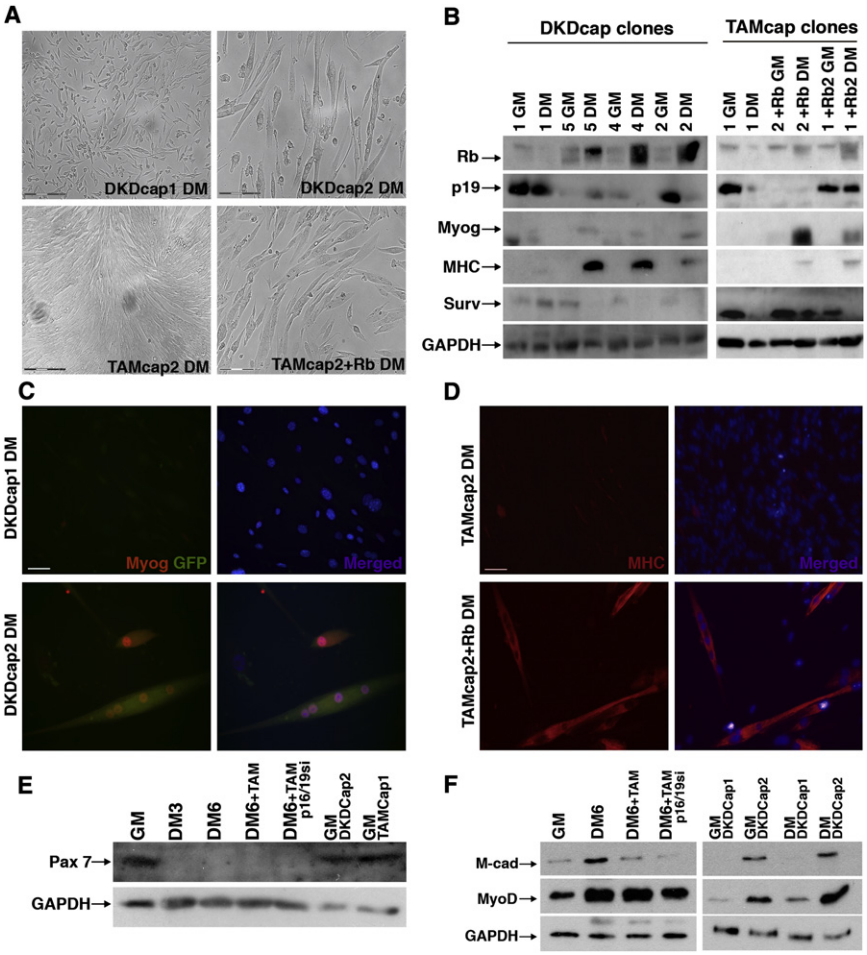

Figure 6. Dedifferentiated Myocytes Are Capable of Expansion and Redifferentiation into Mature Myotubes

(A) Phase contrast images of Rbsi and p16/19si double-knockdown captured (DKDcap) myocyte colonies and TAM with p16/19si-captured myocyte (TAMcap) colonies at DM4, prior to protein harvest for expression analysis. Scale bars represent 150 μm.

(B) Western blot analysis of captured colonies in GM and DM arranged from left to right according to their differentiated morphologies in DM4; protein levels of Rb (100 kDa), p19ARF (20 kDa), myogenin (36 kDa), MHC (220 kDa), and Survivin (20 kDa) as well as GAPDH (35 kDa) as a loading control.

(C) Representative images of two DKDcap myocyte colonies in DM4, labeled for GFP (green) and myogenin (red) as well as Hoechst 33258 (blue). Scale bar represents 25 μm.

(D) Representative images of TAMcap myocyte colony in DM4 labeled for MHC (red) and Hoechst 33258 (blue), a portion of which (bottom) was infected with retrovirus reintroducing Rb expression. Scale bar represents 50 μm.

(E) Western blot analysis of Pax-7 protein (57 kDa) levels in muscle cells in GM, DM at indicated time points and with indicated treatments, and in the DKDcap dedifferentiated clones.

(F) Western blot analysis of M-cadherin protein (88 kDa) and MyoD (34 kDa) levels in primary muscle cells under growth conditions (GM), differentiated conditions (DM6) with indicated treatments, and in the isolated dedifferentiated clones (DKDcap1 and DKDcap2) in GM and DM4 (DM).

Rb and *Ink4a* genes were silenced under conditions of greater survival (Figure S5C) exhibited a high frequency of 28.8% colony formation (Figure 5E).

Redifferentiation of Captured Myocyte Colonies after Exposure to Low Serum

Dedifferentiated muscle cells in axolotls have been shown to be capable of proliferation and contribution to regenerating muscle, although single cell tracking via genetic marking has not been possible to date. After LPC capture, TAM- and p16/19si-treated myocytes proliferated rapidly in GM, and most of the cells lost *myogenin* expression after 72 hr, evidenced by lack of GFP (Figure S6B). To determine whether such dedifferentiated, actively dividing mammalian myocytes were capable of redifferentiation, we exposed these cells to differentiation conditions. However, they continued to proliferate and never fused (Figure S6B, lower panels), by comparison with control LPC-captured myoblasts, which had started to fuse by 3 days in DM (Figure S6A). This lack of differentiation is expected because the TAM-treated cells had permanently lost *Rb* expression. In contrast, Rb suppression in DKD-captured myocytes was transient. Four colonies derived from single DKD-treated captured myocytes were expanded, exposed to DM for 4 days, and then assayed for muscle markers, either by microscopy or biochemically. The DKD colonies spanned the spectrum of differentiation potential, as shown in the top panels of Figures 6A and 6C. One colony (DKDcap1) continued to proliferate despite being in DM whereas another (DKDcap2) differentiated and fused. Heterogeneity in the behavior of captured cells after transient knockdown may be due to clonal variability after extensive proliferation.

Analysis of captured DKD colonies supports a function for pRb in successful redifferentiation, because we found that DKDcap1 cells lost pRb expression, whereas the colonies that readily fused and differentiated (DKDcap4 and DKDcap2) expressed high levels of pRb in DM (Figure 6B). p19ARF expression in DKDcap1 was high, the cells failed to upregulate GFP, and endogenous Myogenin remained undetectable in DM (Figure 6C). In contrast, in the colonies that differentiated well, downregulation of p19ARF was observed in DM. Expression of GFP, Myogenin, and MHC provided confirmation of differentiation

(E) Histogram represents percentage of colony formation after PALM LPC cell isolation after FACS isolation of GFP$^+$ myocyte population as indicated by the scheme in Figure S5A. Error bars indicate the mean ± SE of at least four independent experiments, in which at least 50 membranes were captured for each myocyte trial. Primary muscle cells were differentiated for 4 days (DM4) at the time of LPC isolation.

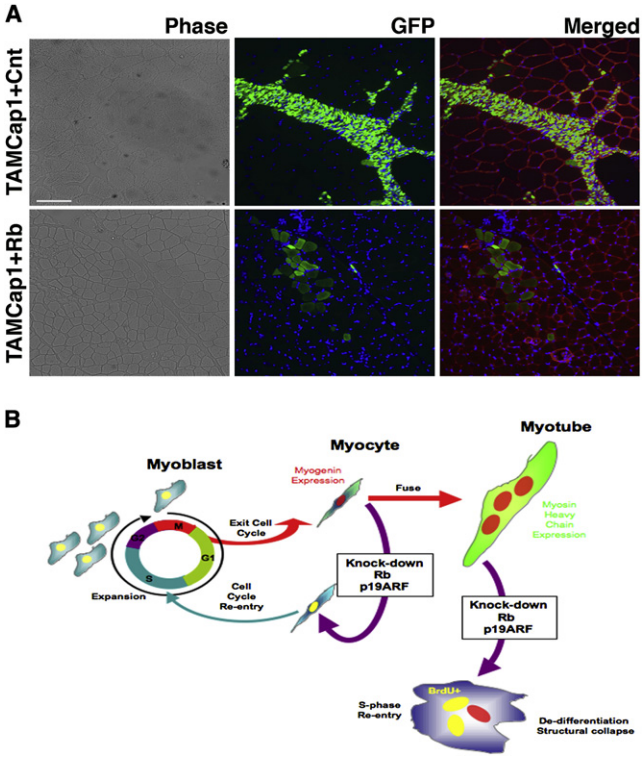

Figure 7. Dedifferentiated Myocytes Are Capable of Fusing to Muscle In Vivo

(A) Representative cross-sections of tibialis anterior 10 days postinjection of 2.5×10^5 cells from TAMcap1 and TAMcap1+Rb clonally expanded myocytes (see Figure 6). Incorporation of dedifferentiated myocytes into pre-existing fibers can be visualized in merged fields by GFP^+ staining (green) of laminin-bound fibers (red), nuclei (blue); to enhance visualization, cells were infected with a constitutive-eGFP expressing retroviral vector prior to injection (n = 4, 3 of which had GFP^+ fibers detected). Scale bar represents 50 μm.

(B) Schematic representation of the events after suppression of Rb and p19ARF in primary differentiated myocytes and multinucleated myotubes.

potential of clones DKDcap4 and DKDcap2 (Figures 6B and 6C). The relative changes in expression patterns of pRb, Ink4a, and myogenic proteins by the DKDcap2 colony and by captured myoblasts were similar (Figures S6C and S6D).

We reasoned that if pRb was reintroduced into the TAM- and p16/19si-captured cells, redifferentiation and fusion should occur. Therefore, we infected a subset of captured colonies with a pMIG retrovirus vector expressing the human *RB* cDNA (Sage et al., 2000). We monitored the TAMcap myoblast colonies after infection with pMIG-*RB* or control pMIG retrovirus and determined that differentiation and fusion occurred in those colonies that re-expressed pRB (Figure 6A, bottom). Analysis of pRB protein levels showed the expected increase in pRB protein that paralleled the upregulation of the myogenic proteins, myogenin, and MHC (Figure 6B). In addition, Survivin levels decreased in the TAMcap1 colony after pMIG-Rb infection (Figure 6B, lane 6). However, ARF levels remained variable among clones. The myogenic potential of TAMcap colonies infected with pMIG-*RB* was also verified by immunofluorescence for MHC (Figure 6D). Together, these data demonstrate that dedifferentiated myocytes are capable of successful redifferentiation in vitro after capture and expansion and that this process is dependent upon expression of *Rb*.

Muscle stem cells and proliferating primary myoblasts express the marker Pax7 (Chargé and Rudnicki, 2004). We tested whether muscle cells with reduced *Rb* and *ink4a* dedifferentiated to a point such that expression of Pax7 was reactivated. Primary myoblasts expressed Pax7 when they were proliferating under growth conditions, but once in differentiation media for at least 72 hr, Pax7 protein levels decreased and remained undetectable by western analysis in mature myotubes (Figure 6E, lanes 2 and 3). After reduction of pRb and ARF, dedifferentiating *myotubes* did not re-express Pax7 (Figure 6E, lanes 4 and 5); however, myocytes from the PALM-captured myogenin-positive population re-expressed Pax7 once they established colonies in conditioned growth media (Figure 6E, lanes 6 and 7). We also tested expression of MyoD and M-cadherin, which have characteristic expression patterns during muscle differentiation. Reduction of pRb and Arf caused a decrease of MyoD and M-cadherin protein levels in myotubes (Figure 6F, left, and Figure S6E). In PALM-generated clones, expression of MyoD and M-cadherin, like morphological differentiation, was correlated with expression of Rb (Figure 6F, right). Only clones that expressed pRb (DKDCap2) expressed relatively high levels of MyoD and M-cadherin, both of which increased somewhat during differentiation (Figure 6F, right, lanes 2 and 4). By contrast, the clone that did not express pRb (DKDCap1), possibly resulting from mutation or deletion during clonal selection, did not express detectable levels of M-cadherin and expressed only low levels of MyoD in growth and differentiation medium (Figure 6F, right, lanes 1 and 3).

Taken together, these results strongly support a role for *Rb* and *Ink4a* in the maintenance of myogenic differentiation, because their suppression in myogenin-expressing postmitotic myocytes leads to division, expansion, and reactivation of Pax7, as well as MyoD and m-cadherin expression patterns consistent with myoblasts.

Captured and Expanded Myocytes Are Capable of Contribution to Muscle In Vivo

Finally, we tested whether PALM LPC-isolated, expanded myocytes could contribute to existing muscle in vivo. 1.5×10^5 DKD-derived dedifferentiated myocytes (DKDcap1 and DKDcap2) were injected into the tibialis anterior (TA) of NOD/SCID mice. *Myogenin-GFP* expression was used to track the injected cells, because this marker was reliably detected in vitro upon differentiation (Figure 6C). Ten days after injection, DKDcap1 cells, which exhibited no fusion in vitro, proliferated excessively in vivo and caused severe disruption of the muscle laminin network at the site of injection (Figure S7, top). On the other hand, DKDcap2 cells readily fused to the existing muscle fibers and caused no disruption of the laminin network (Figure S7, bottom).

We also analyzed in vivo contribution of colonies in which *Rb* was deleted and *ARF* suppressed (TAMcap). Infection with pMIG-*RB* restored RB expression and pLE-GFP retrovirus was used to enhance visualization by expressing GFP constitutively and at higher levels than those produced by the myogenin reporter. Control TAMcap1 cells, which received control pMIG and pLE-GFP infections, proliferated excessively in vivo (Figure 7A, top). By contrast, TAMcap1 cells with reintroduced RB expression efficiently fused to existing muscle fibers, brightly

labeling them with GFP, without any apparent proliferation and without disruption of the existing laminin network (Figure 7A, bottom). We conclude that if pRb expression is either transiently suppressed or adequately restored, dedifferentiated myocytes are capable of redifferentiation and incorporation by fusion to existing muscle in vivo.

DISCUSSION

The molecular basis for the extraordinary disparity between mammals and certain lower vertebrates, such as newts, axolotls, and zebrafish, in their capacity to regenerate injured or amputated tissues remains a major unresolved biological question. Mammalian regeneration of a muscle occurs only if that muscle is replaced after mincing or grafting of small muscles, or when chemical agents spare stem cells. Experiments of this type indicate that significant architectural remodeling can occur in lieu of scarring but that the extent of regeneration is limited by the amount of replaced or surviving muscle (Carlson, 2003). Although endogenous muscle stem cells can account for some degree of regeneration (Collins and Partridge, 2005; Sacco et al., 2008), they do not seem to suffice in extreme circumstances. Indeed, to date there is no evidence that the extensive regeneration of entire muscles seen in urodeles can be achieved by any known mammalian mechanism when a significant mass of tissue is removed and not replaced. This regenerative potential is probably limited in part by a combination of excessive demand for cell proliferation at the site of injury in order to replace lost tissue, and an inhibition of architectural remodeling by fibrosis. A possible basis for the failure of regeneration in mammals, which has fascinated scientists for centuries, is a capacity that regenerative vertebrates have retained and mammals have lost: dedifferentiation.

Does dedifferentiation endow regenerative vertebrates with capabilities that mammals lack? This question underscores the need for novel insights into the molecular mechanisms of dedifferentiation in order to discover what is missing in mammals. In urodeles, compelling evidence from studies of skeletal muscle suggests that dedifferentiation is a major mode of tissue regeneration (Hay and Fischman, 1961; Lentz, 1969; Kintner and Brockes, 1984; Lo et al., 1993; Tanaka et al., 1997; Echeverri et al., 2001). Dedifferentiation involves two processes, which are separable and independent: muscle cell fragmentation into individual mononuclear cells and cell cycle re-entry followed by proliferation (Velloso et al., 2000; Brockes and Kumar, 2008). In mammalian myotubes produced with the immortalized cell line C2C12, overexpression of transcriptional factors present in the blastema such as *msx1* (Odelberg et al., 2000) or *twist* (Hjiantoniou et al., 2008), or exposure to small molecules that disrupt the cytoskeleton, have been reported to result in myotube fragmentation (Perez et al., 2002). In the dedifferentiation studies reported here, fragmentation of muscle cells was not observed, which is in good agreement with reports showing that the fragmentation process in urodeles is independent of cell cycle reentry (Velloso et al., 2000). In addition, because the trigger and mechanism for muscle fragmentation and cellularization in urodeles remains unknown, it is currently not possible to determine whether a similar pathway exists in mammals. Understanding how fragmentation occurs and delineating the dedifferentiation mechanisms are complementary but distinct goals in muscle regeneration biology.

Molecular Regulation of Dedifferentiation by *Rb* and *ARF*

Our decision to suppress *Rb* in experiments directed at elucidating the mechanisms underlying muscle dedifferentiation was based on evidence in urodeles that pRb coordinates muscle cell cycle entry in response to damage (Tanaka et al., 1997). In mammals as in urodeles, cell cycle regulation by pRb is dynamic and controlled primarily by its phosphorylation state (Lipinski and Jacks, 1999; Burkhart and Sage, 2008). There is also a wealth of data firmly establishing the tumor suppressor Rb as a necessary player in the orchestration of mammalian muscle cell differentiation, including evidence for a dual role in both muscle cell cycle progression and exit (Gu et al., 1993; Zacksenhaus et al., 1996; Puri et al., 2001; Blais et al., 2007). Indeed, *Rb* null mice die before birth and lack differentiated muscles (Zacksenhaus et al., 1996; Takahashi et al., 2003). Furthermore, pRb has also been shown to act not only as a cell cycle regulator, but also to impact differentiation and tissue-specific gene expression directly by binding histone deacetylase 1 (HDAC1) and promoting activation of muscle genes such as MyoD (Puri et al., 2001). Once differentiation occurs, this state is stably maintained, at least in mammals. This stability is underscored by the inability to reverse differentiation simply by inactivating pRb in primary differentiated mammalian muscle cells (Camarda et al., 2004; Huh et al., 2004). Indeed, studies reporting otherwise have been confounded by the use of immortalized cell lines such as C2C12 (Gu et al., 1993; Blais et al., 2007), which we show here have a deletion in the *ink4a* locus and therefore do not express the *ink4a* products. Loss or suppression of *Rb* leads only to moderate dedifferentiation, as demonstrated by the reduced accumulation of myogenin and MHC (Figure 3). In fact, as shown in this report and by others previously (Camarda et al., 2004; Huh et al., 2004), it is remarkable how little phenotypic change occurs in primary differentiated skeletal muscle cells when *Rb* is suppressed.

The minimal impact of pRb absence alone on muscle dedifferentiation suggested that maintenance of mammalian differentiation is ensured by a separate mechanism. Whereas the basal *Rb* and *p53* pathways are functional in lower vertebrates, we reasoned that a modulator that is absent in regeneration-competent vertebrates would be a good candidate regeneration suppressor in mammals. We therefore focused on the *ink4a* locus and *ARF* in particular. Unlike *Rb*, inactivation of *ARF* alone in knockout mice has no apparent effect on differentiation (Serrano et al., 1996; Kamijo et al., 1997). In agreement with these reports, we found that suppressing *ARF* alone had no effect on muscle differentiation or dedifferentiation. Loss of *Rb* led to elevated expression and protein levels of ARF. Concomitant inactivation of *Rb* and *ARF* caused extensive loss of differentiation. Previously differentiated myotubes exhibited robust DNA synthesis and expression of mitotic proteins upon acute loss of *Rb* and p19ARF, suggesting that these two are nodal points for intrinsic control of muscle cell cycle reentry. The profound loss of architectural integrity and downregulation of myogenin, MRF-4, MHC, and M-CK, further suggests that pRb and ARF together are potent stabilizers of the differentiated state. Notably, alternative approaches to induce cycling by altering growth factor signaling and regeneration in mammalian

cardiac muscle cells (Bersell et al., 2009) produce a very moderate effect when compared to regenerating urodele muscle. We speculate that ARF may inhibit robust cycling and regeneration in this setting as well.

Our findings support the hypothesis that tumor suppression mediated by the *ink4a* locus arose at the expense of regeneration. Both *p16ink4a* and *p19ARF* have been recently shown to contribute to the decline in regenerative potential of multiple tissues during aging by affecting stem cell self-renewal (Sharpless and DePinho, 2007; Levi and Morrison, 2008). Our study suggests that the *ink4a* locus has an additional negative impact on tissue regeneration, i.e., suppression of cell cycle reentry and dedifferentiation. The remarkable combined effect of acute *Rb* and *ARF* loss strongly suggests (1) that continuous expression of pRb itself has an important function in maintaining the differentiated state and (2) that the maintenance of the differentiated state in mammals depends on complementary activities of pRb and ARF. These findings are explicable in view of the known need for continuous regulation of differentiation (Blau and Baltimore, 1991; Yamanaka and Blau, 2010) as well as the documented functions of Rb and ARF in preventing inappropriate cycling as tumor suppressors.

Single Cell Analyses of Reversal of Differentiation

Bulk cultures do not allow a definitive assessment that a given cell has divided. The lack of transgenic animals, cellular complexity, and rapid developmental changes observed in the blastema has hindered analysis of dedifferentiation at the single cell level in urodele regeneration until recently (Sobkow et al., 2006). In mammalian muscle culture systems in which S phase reentry was observed, the persistence of cells at earlier stages of differentiation cannot be ruled out (Gu et al., 1993; Schneider et al., 1994; Blais et al., 2007). In addition, continuous time-lapse monitoring (Duckmanton et al., 2005) and single cell analysis are essential, because reports of division of differentiated muscle cells could be the result of cell migration. To overcome these problems, we employed (1) dynamic single-cell tracking of myocytes isolated in microwells by time-lapse microscopy and (2) isolation of single myocytes by PALM laser capture microscopy. In particular, the laser microsdissection and catapulting technology allows for unambiguous documentation of the division of individual differentiated cells, as shown by the fact that they are each selected and isolated on the basis of both their morphology and their expression of a genetic marker of differentiation, myogenin. These single cell studies clearly demonstrated that cell cycle entry and expansion of individual differentiated postmitotic myocytes occurs after *Rb* and *p19ARF* loss. By contrast, untreated myocytes crawled off of membranes, but never divided. We further demonstrated the regenerative potential of dedifferentiated myocytes by inducing redifferentiation. A subset of captured colonies produced by transient inactivation of *Rb* and *p19ARF* were exposed to differentiation medium in culture and fused to form myotubes. Additionally, in myocytes that had irreversibly lost *Rb* expression resulting from Cre-mediated excision, reintroduction of *RB* by retroviral delivery not only induced myotube formation and muscle gene expression in vitro, but also resulted in fusion and regeneration of myofibers in vivo with typical architecture and no evidence of the tumorigenic characteristics of cells that did not receive *RB*. These findings suggest that transient inactivation of the two tumor suppressors could yield dedifferentiated cells with extensive regenerative potential as depicted in the diagram in Figure 7B.

We capitalized on evolutionary differences to genetically modify the mammalian cell cycle regulatory pathways to more closely mimic those found in lower vertebrates. Our results reveal that it is possible to derive regenerative cells from differentiated, postmitotic muscle in addition to classically defined stem cells. Skeletal muscle cells can alternate between a differentiated, postmitotic state and a proliferative, regenerative state, retaining the essential characteristics of their cell type of origin during the regenerative cycle. Our experiments implicate ARF in the suppression of regeneration in mammalian cells by impeding dedifferentiation. We postulate that a combination of *transient* interventions to inactivate the *Rb* pathway while suppressing *ARF* may be fruitfully employed to maximize a mammalian regenerative response.

EXPERIMENTAL PROCEDURES

Mice and Primary Myoblast Preparation

Rosa26-CreERT2 Rblox/lox mice (Viatour et al., 2008) were crossed to mice carrying a Cre-responsive β-galactosidase reporter allele (Ventura et al., 2007). The hind leg muscles of 6- to 8-week-old offspring were prepared for primary myoblast harvest as described (Rando and Blau, 1994). All animal experiments were performed in accordance with Stanford University animal use protocols.

Cell Culture

C2C12 and primary mouse myoblasts were cultured as described in Pajcini et al. (2008) and Supplemental Experimental Procedures.

Cloning and Vector Construction

pLE-myog3R-GFP retroviral vector was constructed by subcloning the myogenin promoter elements driving GFP expression from peGFPN1-hmyg (a gift from Daniel Kemp-Novartis) into the pLE-GFP vector. See Supplemental Experimental Procedures for details of the construct preparation and virus production.

siRNA Silencing and Semiquantitative RT-PCR

RNA interference was carried out with small-interfering RNA duplexes designed then screened for specific and effective knockdown of target genes. Duplexes were designed for *p16/19* sense sequence AGGUGAUGAUGAU GGGCAAUU and *p19ARF* sense sequence GCUCUGGCUUUCGUGAACAUG or ordered directly as ON-TARGETplus siRNA Rb1 (J-047474-06) from Thermo/Dharmacon. For control transfections, nontargeting siRNA#1 (D-001810-01-05) and siGlo-Green were purchased from Thermo/Dharmacon. Transfections of siRNA duplexes, resuspended in siRNA buffer (Dharmacon), were carried out after differentiation of myocytes or after fusion of myotubes at 48–72 hr in DM with siImporter transfection reagent (Millipore) as per manufacturer's instructions. Transfection mix was added to cells after supplemented to differentiation media for 12 hr. RNA was harvested from C2C12 or primary cells in GM or DM by RNeasy mini kit (QIAGEN) and 200 ng of total RNA was used in semiquantitative RT-PCR analysis with Superscript III One-Step RT-PCR (invitrogen). Primers designed for genes tested and details of the PCR reactions may be found in Supplemental Experimental Procedures.

BrdU Analysis

5-bromo-2′-deoxy-uridine (BrdU) labeling and detection kit (Roche) was used according to the manufacturer's instructions. BrdU labeling reagent was added to the cells with fresh DM media for 12 hr.

Western Analysis

Cells were lysed at room temperature in lysis buffer (50 mM Tris [pH 7.5], 10 mM $MgCl_2$, 0.3 M NaCl, 2% IGEPAL). When necessary, membranes were

stripped by incubating at 50°C for 45 min and then 1 hr at RT in stripping buffer (100 mM 2-mercaptoethanol, 2% SDS, 62 mM Tris [pH 7]).

See Supplemental Experimental Procedures for details of antibody use.

Immunofluorescence

C2C12 myotubes and primary myocytes or myotubes seeded densely for fusion or sparsely for differentiation as described above were fixed and permeabilized as per manufacturer's instructions when costaining with BrdU or with 1.5% paraformaldehyde 15 min at room temperature (RT) then permeabilized with 0.3% Triton-PBS 10 min at RT. See Supplemental Experimental Procedures for details of antibody use.

Cells were imaged with Zeiss Axioplan2 with 40× water immersion objective, Zeiss Axiovert 200M, or Zeiss Observer Z1 with NeoFluar 10× or LD Plan NeoFluar 20× objectives while ORCA-ER C4742-95; Hamamatsu Photonics, or Axiocam MRm cameras were used to capture images. Openlab 5.0.2, Volocity 3.6.1 (Improvision), and PALM Robo V4 (Zeiss) were the software used for image acquisition. Images were composed and edited in Photoshop CS (Adobe). Background was reduced with contrast adjustments and color balance was performed to enhance colors. All modifications were applied to the entire image.

FACS Sorting

Cells were harvested from culture dishes after 0.05% trypsin treatment, centrifuged, resuspended in FACS buffer (PBS + 2% GS + 2 mM EDTA), and kept on ice until analysis. Cells were analyzed and sorted with a FACSVantage SE (BD Biosciences), with the DIVA analysis software. Dead cells were gated out by staining with PI (1 μg/ml), and cells were sorted for GFP expression at low pressure to preserve cell viability. Double sort was carried out in order to obtain a purity of 99% viable cells. In the second sort, cells were sorted directly in GM or DM as indicated and then seeded in different platforms (microwells or PALM duplex dishes).

PALM LPC

Primary myoblasts were sparsely seeded for differentiation in 50 mm or 35 mm laminin (Roche) -coated Duplexdishes (Zeiss). See Supplemental Experimental Procedures for details. Laser ablation was carried out after stage calibration, laser focus, and optical focus calibration as per manufacturer's instructions, in a Zeiss Observer Z1 inverted microscope outfitted with PALM Microbeam (Zeiss). Ablated membranes were catapulted by LPC bursts into Roboarm SingleTube Capture II receptacles (500 μl eppendorf tube cap) with 80 μl of media. Membrane/myocyte capture was verified after capture by direct observation of the captured receptacle. Total volume of the receptacle was transferred into 12- or 24-well collagen-coated plates, where captured myocytes were cultured in conditioned growth media (cGM), which was harvested from actively dividing myoblasts and 0.2 μm filtered.

Immunocytochemistry

10 days after injection, TA muscles were dissected and immersed in PBS/0.5% EM-grade PFA (Polysciences) for 2 hr at RT followed by overnight immersion in PBS with 20% sucrose at 4°C. Section staining and image analysis was performed as described in Pajcini et al. (2008).

Time-Lapse Microscopy

Primary myotubes were imaged with Zeiss Axiovert 200M equipped with time-lapse apparatus CTI-Controller 3700 Digital; Tempcontrol 37-2 digital; scanning stage Incubator XL 100/135 (PECON). Frames were captured every 10 min for a total of 50 hr, encompassing days 5 and 6 during primary myotube fusion and maturation. Images were acquired and analyzed with Volocity 3.6.1 (Improvision).

SUPPLEMENTAL INFORMATION

Supplemental Information includes seven figures and two movies and can be found with this article online at doi:10.1016/j.stem.2010.05.022.

ACKNOWLEDGMENTS

We would like to thank Alessandra Sacco for TA injections and numerous helpful discussion on this manuscript; Daniel Kemp (Novartis) for providing us with the peGFPN1-hmyg plasmid from which the myogenin promoter elements were subcloned; Rainer Gangnus and Renate Burgemeister from Carl Zeiss MicroImaging GmbH for invaluable help in PALM LPC methodology; Justine Seidenfeld for her early work on the project; Karen Havenstrite and Penney Gilbert for microwell array construction; Rose Tran for sectioning; and Warren Pear for use of laboratory facilities.

We gratefully acknowledge grants 2T32 HD007249 of The Developmental and Neonatal Biology Program and NIH training grants 5T32 AI07328 and 5T32 HD007249 to K.V.P.; grant F32 AR051678-01 to J.H.P.; and NIH grants AG009521, AG020961, HL096113, MDA grant 4320, LLS grant TR6025-09, JDRF grant 34-2008-623, CIRM grant RT1-01001, and the Baxter Foundation to H.M.B.

Received: January 29, 2010
Revised: April 29, 2010
Accepted: May 26, 2010
Published: August 5, 2010

REFERENCES

Bartolini, F., and Gundersen, G.G. (2006). Generation of noncentrosomal microtubule arrays. J. Cell Sci. *119*, 4155–4163.

Bersell, K., Arab, S., Haring, B., and Kühn, B. (2009). Neuregulin1/ErbB4 signaling induces cardiomyocyte proliferation and repair of heart injury. Cell *138*, 257–270.

Blais, A., van Oevelen, C.J., Margueron, R., Acosta-Alvear, D., and Dynlacht, B.D. (2007). Retinoblastoma tumor suppressor protein-dependent methylation of histone H3 lysine 27 is associated with irreversible cell cycle exit. J. Cell Biol. *179*, 1399–1412.

Blau, H.M., and Baltimore, D. (1991). Differentiation requires continuous regulation. J. Cell Biol. *112*, 781–783.

Blau, H.M., Pavlath, G.K., Hardeman, E.C., Chiu, C.P., Silberstein, L., Webster, S.G., Miller, S.C., and Webster, C. (1985). Plasticity of the differentiated state. Science *230*, 758–766.

Brockes, J.P., and Kumar, A. (2008). Comparative aspects of animal regeneration. Annu. Rev. Cell Dev. Biol. *24*, 525–549.

Brookes, S., Rowe, J., Gutierrez Del Arroyo, A., Bond, J., and Peters, G. (2004). Contribution of p16(INK4a) to replicative senescence of human fibroblasts. Exp. Cell Res. *298*, 549–559.

Burkhart, D.L., and Sage, J. (2008). Cellular mechanisms of tumour suppression by the retinoblastoma gene. Nat. Rev. Cancer *8*, 671–682.

Caldas, H., Jiang, Y., Holloway, M.P., Fangusaro, J., Mahotka, C., Conway, E.M., and Altura, R.A. (2005). Survivin splice variants regulate the balance between proliferation and cell death. Oncogene *24*, 1994–2007.

Camarda, G., Siepi, F., Pajalunga, D., Bernardini, C., Rossi, R., Montecucco, A., Meccia, E., and Crescenzi, M. (2004). A pRb-independent mechanism preserves the postmitotic state in terminally differentiated skeletal muscle cells. J. Cell Biol. *167*, 417–423.

Carlson, B.M. (2003). Muscle regeneration in amphibians and mammals: Passing the torch. Dev. Dyn. *226*, 167–181.

Chargé, S.B., and Rudnicki, M.A. (2004). Cellular and molecular regulation of muscle regeneration. Physiol. Rev. *84*, 209–238.

Collins, C.A., and Partridge, T.A. (2005). Self-renewal of the adult skeletal muscle satellite cell. Cell Cycle *4*, 1338–1341.

Crescenzi, M., Soddu, S., Sacchi, A., and Tatò, F. (1995). Adenovirus infection induces reentry into the cell cycle of terminally differentiated skeletal muscle cells. Ann. N Y Acad. Sci. *752*, 9–18.

DeGregori, J., Leone, G., Miron, A., Jakoi, L., and Nevins, J.R. (1997). Distinct roles for E2F proteins in cell growth control and apoptosis. Proc. Natl. Acad. Sci. USA *94*, 7245–7250.

Duckmanton, A., Kumar, A., Chang, Y.T., and Brockes, J.P. (2005). A single-cell analysis of myogenic dedifferentiation induced by small molecules. Chem. Biol. *12*, 1117–1126.

Echeverri, K., Clarke, J.D., and Tanaka, E.M. (2001). In vivo imaging indicates muscle fiber dedifferentiation is a major contributor to the regenerating tail blastema. Dev. Biol. *236*, 151–164.

Gardiner, D.M., and Bryant, S.V. (1996). Molecular mechanisms in the control of limb regeneration: The role of homeobox genes. Int. J. Dev. Biol. *40*, 797–805.

Gilley, J., and Fried, M. (2001). One INK4 gene and no ARF at the Fugu equivalent of the human INK4A/ARF/INK4B tumour suppressor locus. Oncogene *20*, 7447–7452.

Gu, W., Schneider, J.W., Condorelli, G., Kaushal, S., Mahdavi, V., and Nadal-Ginard, B. (1993). Interaction of myogenic factors and the retinoblastoma protein mediates muscle cell commitment and differentiation. Cell *72*, 309–324.

Hay, E.D., and Fischman, D.A. (1961). Origin of the blastema in regenerating limbs of the newt Triturus viridescens. An autoradiographic study using tritiated thymidine to follow cell proliferation and migration. Dev. Biol. *3*, 26–59.

Hickson, G.R., and O'Farrell, P.H. (2008). Anillin: A pivotal organizer of the cytokinetic machinery. Biochem. Soc. Trans. *36*, 439–441.

Hjiantoniou, E., Anayasa, M., Nicolaou, P., Bantounas, I., Saito, M., Iseki, S., Uney, J.B., and Phylactou, L.A. (2008). Twist induces reversal of myotube formation. Differentiation *76*, 182–192.

Huh, M.S., Parker, M.H., Scimè, A., Parks, R., and Rudnicki, M.A. (2004). Rb is required for progression through myogenic differentiation but not maintenance of terminal differentiation. J. Cell Biol. *166*, 865–876.

Kamijo, T., Zindy, F., Roussel, M.F., Quelle, D.E., Downing, J.R., Ashmun, R.A., Grosveld, G., and Sherr, C.J. (1997). Tumor suppression at the mouse INK4a locus mediated by the alternative reading frame product p19ARF. Cell *91*, 649–659.

Kazianis, S., Morizot, D.C., Coletta, L.D., Johnston, D.A., Woolcock, B., Vielkind, J.R., and Nairn, R.S. (1999). Comparative structure and characterization of a CDKN2 gene in a *Xiphophorus* fish melanoma model. Oncogene *18*, 5088–5099.

Kim, S.H., Mitchell, M., Fujii, H., Llanos, S., and Peters, G. (2003). Absence of p16INK4a and truncation of ARF tumor suppressors in chickens. Proc. Natl. Acad. Sci. USA *100*, 211–216.

Kintner, C.R., and Brockes, J.P. (1984). Monoclonal antibodies identify blastemal cells derived from dedifferentiating limb regeneration. Nature *308*, 67–69.

Kobayashi, K., Hatano, M., Otaki, M., Ogasawara, T., and Tokuhisa, T. (1999). Expression of a murine homologue of the inhibitor of apoptosis protein is related to cell proliferation. Proc. Natl. Acad. Sci. USA *96*, 1457–1462.

Kragl, M., Knapp, D., Nacu, E., Khattak, S., Maden, M., Epperlein, H.H., and Tanaka, E.M. (2009). Cells keep a memory of their tissue origin during axolotl limb regeneration. Nature *460*, 60–65.

Lassar, A., and Münsterberg, A. (1994). Wiring diagrams: Regulatory circuits and the control of skeletal myogenesis. Curr. Opin. Cell Biol. *6*, 432–442.

Lentz, T.L. (1969). Cytological studies of muscle dedifferentiation and differentiation during limb regeneration of the newt *Triturus*. Am. J. Anat. *124*, 447–479.

Levi, B.P., and Morrison, S.J. (2008). Stem cells use distinct self-renewal programs at different ages. Cold Spring Harb. Symp. Quant. Biol. *73*, 539–553.

Li, F., and Altieri, D.C. (1999). Transcriptional analysis of human survivin gene expression. Biochem. J. *344*, 305–311.

Lipinski, M.M., and Jacks, T. (1999). The retinoblastoma gene family in differentiation and development. Oncogene *18*, 7873–7882.

Lo, D.C., Allen, F., and Brockes, J.P. (1993). Reversal of muscle differentiation during urodele limb regeneration. Proc. Natl. Acad. Sci. USA *90*, 7230–7234.

Lutolf, M.P., Doyonnas, R., Havenstrite, K., Koleckar, K., and Blau, H.M. (2009). Perturbation of single hematopoietic stem cell fates in artificial niches. Integr Biol (Camb) *1*, 59–69.

Molkentin, J.D., and Olson, E.N. (1996). Defining the regulatory networks for muscle development. Curr. Opin. Genet. Dev. *6*, 445–453.

Novitch, B.G., Mulligan, G.J., Jacks, T., and Lassar, A.B. (1996). Skeletal muscle cells lacking the retinoblastoma protein display defects in muscle gene expression and accumulate in S and G2 phases of the cell cycle. J. Cell Biol. *135*, 441–456.

Odelberg, S.J., Kollhoff, A., and Keating, M.T. (2000). Dedifferentiation of mammalian myotubes induced by msx1. Cell *103*, 1099–1109.

Pajcini, K.V., Pomerantz, J.H., Alkan, O., Doyonnas, R., and Blau, H.M. (2008). Myoblasts and macrophages share molecular components that contribute to cell-cell fusion. J. Cell Biol. *180*, 1005–1019.

Perez, O.D., Chang, Y.T., Rosania, G., Sutherlin, D., and Schultz, P.G. (2002). Inhibition and reversal of myogenic differentiation by purine-based microtubule assembly inhibitors. Chem. Biol. *9*, 475–483.

Poss, K.D., Wilson, L.G., and Keating, M.T. (2002). Heart regeneration in zebrafish. Science *298*, 2188–2190.

Puri, P.L., Iezzi, S., Stiegler, P., Chen, T.T., Schiltz, R.L., Muscat, G.E., Giordano, A., Kedes, L., Wang, J.Y., and Sartorelli, V. (2001). Class I histone deacetylases sequentially interact with MyoD and pRb during skeletal myogenesis. Mol. Cell *8*, 885–897.

Rando, T.A., and Blau, H.M. (1994). Primary mouse myoblast purification, characterization, and transplantation for cell-mediated gene therapy. J. Cell Biol. *125*, 1275–1287.

Reimann, J.D., Freed, E., Hsu, J.Y., Kramer, E.R., Peters, J.M., and Jackson, P.K. (2001). Emi1 is a mitotic regulator that interacts with Cdc20 and inhibits the anaphase promoting complex. Cell *105*, 645–655.

Ruchaud, S., Carmena, M., and Earnshaw, W.C. (2007). Chromosomal passengers: Conducting cell division. Natl. Rev. Mol. Cell Biol. *8*, 798–812.

Sacco, A., Siepi, F., and Crescenzi, M. (2003). HPV E7 expression in skeletal muscle cells distinguishes initiation of the postmitotic state from its maintenance. Oncogene *22*, 4027–4034.

Sacco, A., Doyonnas, R., Kraft, P., Vitorovic, S., and Blau, H.M. (2008). Self-renewal and expansion of single transplanted muscle stem cells. Nature *456*, 502–506.

Sage, J., Mulligan, G.J., Attardi, L.D., Miller, A., Chen, S., Williams, B., Theodorou, E., and Jacks, T. (2000). Targeted disruption of the three Rb-related genes leads to loss of G(1) control and immortalization. Genes Dev. *14*, 3037–3050.

Sage, J., Miller, A.L., Pérez-Mancera, P.A., Wysocki, J.M., and Jacks, T. (2003). Acute mutation of retinoblastoma gene function is sufficient for cell cycle re-entry. Nature *424*, 223–228.

Sawin, K.E., and Mitchison, T.J. (1995). Mutations in the kinesin-like protein Eg5 disrupting localization to the mitotic spindle. Proc. Natl. Acad. Sci. USA *92*, 4289–4293.

Schneider, J.W., Gu, W., Zhu, L., Mahdavi, V., and Nadal-Ginard, B. (1994). Reversal of terminal differentiation mediated by p107 in Rb-/- muscle cells. Science *264*, 1467–1471.

Schutze, K., Niyaz, Y., Stich, M., and Buchstaller, A. (2007). Noncontact laser microdissection and catapulting for pure sample capture. Methods Cell Biol. *82*, 649–673.

Serrano, M., Lee, H., Chin, L., Cordon-Cardo, C., Beach, D., and DePinho, R.A. (1996). Role of the INK4a locus in tumor suppression and cell mortality. Cell *85*, 27–37.

Sharpless, N.E., and DePinho, R.A. (1999). The INK4A/ARF locus and its two gene products. Curr. Opin. Genet. Dev. *9*, 22–30.

Sharpless, N.E., and DePinho, R.A. (2007). How stem cells age and why this makes us grow old. Natl. Rev. Mol. Cell Biol. *8*, 703–713.

Shen, X., Collier, J.M., Hlaing, M., Zhang, L., Delshad, E.H., Bristow, J., and Bernstein, H.S. (2003). Genome-wide examination of myoblast cell cycle withdrawal during differentiation. Dev. Dyn. *226*, 128–138.

Sherr, C.J., and DePinho, R.A. (2000). Cellular senescence: Mitotic clock or culture shock? Cell *102*, 407–410.

Sherr, C.J., Bertwistle, D., DEN Besten, W., Kuo, M.L., Sugimoto, M., Tago, K., Williams, R.T., Zindy, F., and Roussel, M.F. (2005). p53-Dependent and -independent functions of the Arf tumor suppressor. Cold Spring Harb. Symp. Quant. Biol. *70*, 129–137.

Sobkow, L., Epperlein, H.H., Herklotz, S., Straube, W.L., and Tanaka, E.M. (2006). A germline GFP transgenic axolotl and its use to track cell fate: dual origin of the fin mesenchyme during development and the fate of blood cells during regeneration. Dev. Biol. *290*, 386–397.

Soriano, P. (1999). Generalized lacZ expression with the ROSA26 Cre reporter strain. Nat. Genet. *21*, 70–71.

Stich, M., Thalhammer, S., Burgemeister, R., Friedmann, G., Ehnle, S., Luthy, C., and Schutze, K. (2003). Live cell catapulting and recultivation. Pathol. Res. Pract. *199*, 4105–4109.

Takahashi, C., Bronson, R.T., Socolovsky, M., Contreras, B., Lee, K.Y., Jacks, T., Noda, M., Kucherlapati, R., and Ewen, M.E. (2003). Rb and N-ras function together to control differentiation in the mouse. Mol. Cell. Biol. *23*, 5256–5268.

Tanaka, E.M., and Weidinger, G. (2008). Micromanaging regeneration. Genes Dev. *22*, 700–705.

Tanaka, E.M., Gann, A.A., Gates, P.B., and Brockes, J.P. (1997). Newt myotubes reenter the cell cycle by phosphorylation of the retinoblastoma protein. J. Cell Biol. *136*, 155–165.

Velloso, C.P., Kumar, A., Tanaka, E.M., and Brockes, J.P. (2000). Generation of mononucleate cells from post-mitotic myotubes proceeds in the absence of cell cycle progression. Differentiation *66*, 239–246.

Velloso, C.P., Simon, A., and Brockes, J.P. (2001). Mammalian postmitotic nuclei reenter the cell cycle after serum stimulation in newt/mouse hybrid myotubes. Curr. Biol. *11*, 855–858.

Ventura, A., Kirsch, D.G., McLaughlin, M.E., Tuveson, D.A., Grimm, J., Lintault, L., Newman, J., Reczek, E.E., Weissleder, R., and Jacks, T. (2007). Restoration of p53 function leads to tumor regression in vivo. Nature *445*, 661–665.

Viatour, P., Somervaille, T.C., Venkatasubrahmanyam, S., Kogan, S., McLaughlin, M.E., Weissman, I.L., Butte, A.J., Passegué, E., and Sage, J. (2008). Hematopoietic stem cell quiescence is maintained by compound contributions of the retinoblastoma gene family. Cell Stem Cell *3*, 416–428.

Walsh, K., and Perlman, H. (1997). Cell cycle exit upon myogenic differentiation. Curr. Opin. Genet. Dev. *7*, 597–602.

Yamanaka, S., and Blau, H.M. (2010). Nuclear reprogramming to a pluripotent state by three approaches. Nature *465*, 704–712.

Zacksenhaus, E., Jiang, Z., Chung, D., Marth, J.D., Phillips, R.A., and Gallie, B.L. (1996). pRb controls proliferation, differentiation, and death of skeletal muscle cells and other lineages during embryogenesis. Genes Dev. *10*, 3051–3064.